Supplementary Material

Tissot *et al*, Large-scale head-to-head comparison of on- and off-target profiles of [^{18}F]Tauvid and [^{18}F]MK6240 tau-PET in aging and Alzheimer's disease.

Supplementary methods:

Dataset:

Data was collected from 681 individuals from the HEAD dataset. HEAD is a multi-site project including seven sites in the United States of America, one site in Canada and one in Spain. More details can be found on https://head-study.info/. The project was approved by Advarra Institutional Review Board in the USA, the Douglas Research Institute Research Ethics Board in Canada, and the ethics committee of the Fundació de Gestió Sanitària Hospital de la Santa Creu i Sant Pau in Spain. Written consent was obtained from participants. All underwent cross-sectional assessments of magnetic resonance imaging (MRI), [^{18}F]Tauvid and [^{18}F]MK6240 tau-PETs, and an Aβ-PET scan (either [^{11}C]PiB, [^{18}F]NAV4694 or [^{18}F]Florbetaben based on availability at the scanning site) and a neuropsychological evaluation. Individuals without objective cognitive impairment (CDR=0 and MMSE>26) were categorized as cognitively unimpaired (CU) young (CUY) if they were ≤ 25 years of age or CU older (CUO) if they were ≥ 50 years of age (1). Diagnosis of mild cognitive impairment (MCI) and Alzheimer's Disease dementia (AD) was assigned by consensus meeting at each site, that reviewed their clinical and neuropsychological assessments. A dedicated team of neurologist, imaging specialists and neuropsychologist was present at each meeting to ensure consistency among research sites. Following McKhann *et al* (2), MCI was defined as subjective and objective decline (CDR of 0.5) and preserved activity of daily living, and dementia met the National Institute of Aging-Alzheimer's Association criteria (NIA-AA), and had CDR scores of 0.5 to 2. Based on the NIA-AA research framework, participants with subjective memory complaints but without a diagnosis of mild cognitive impairment (MCI) or dementia were analyzed together with the CU group (2). Individuals showing cognitive impairment but a negative Aβ-PET status were combined as a cognitively impaired (CI) Aβ- group.

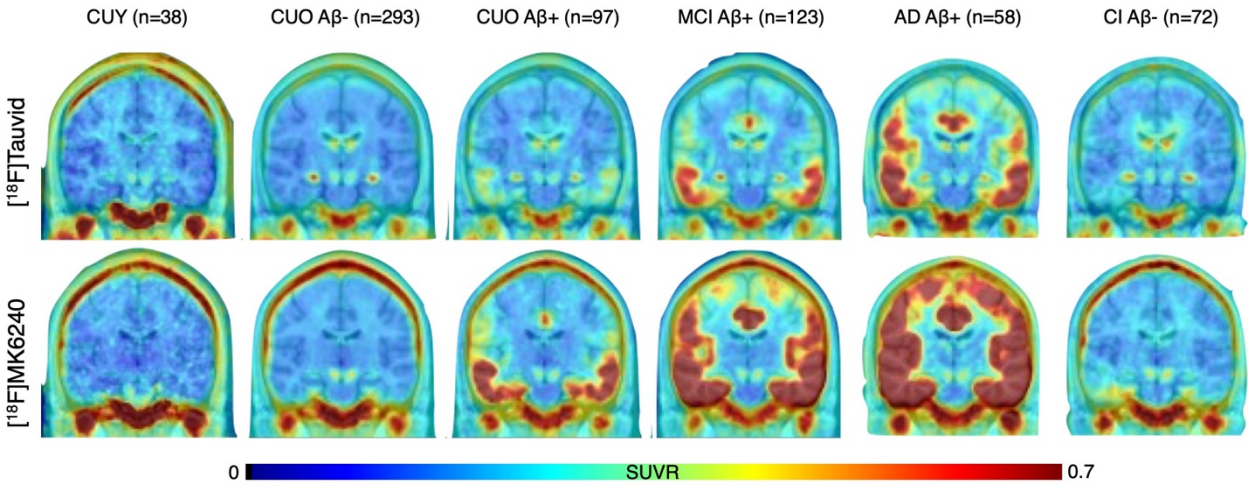
PET processing:

[^{18}F]Tauvid was acquired 80-100 minutes and [^{18}F]MK6240 was acquired 90-110 minutes post-injection, (3). For Aβ-PET scans, images were acquired with acquisition windows post-injection as follows: [^{11}C]PiB (40-60 or 50-70 min), [^{18}F]Florbetaben (90-110 min) and [^{18}F]NAV4694 (50-70 min), based on site availability. Harmonized reconstruction parameters were adopted from ADNI. Individual frames were realigned, averaged, and then coregistered to the individual's T1-weighted MPRAGE structural image. For tau-PET imaging, inferior cerebellar grey was used as the reference region (4, 5) following the Berkeley PET imaging pipeline (BPIP) (6). For Aβ-PET imaging, the whole cerebellum mask was used as the reference region (7). Images were smoothed to achieve a final estimated resolution of 6mm^3 FWHM. The following regions were defined in native space, using co-registered MRI segmented with FreeSurfer. On-target regions were: Braak region of interest (ROI) I to VI, whole cortex and meta-temporal ROI. Braak ROIs were as follows: Braak I (entorhinal cortex), Braak II (hippocampus), Braak III (amygdala, parahippocampal gyrus, fusiform gyrus, lingual gyrus), Braak IV (insula, inferior temporal, lateral temporal, posterior cingulate, and inferior parietal), Braak V (orbitofrontal, superior temporal, inferior frontal, cuneus, anterior cingulate, supramarginal gyrus, lateral occipital, precuneus, superior parietal, superior frontal, rostro medial frontal), and Braak VI (paracentral, postcentral, precentral, and peri-calcarine) (8). For stages III–VI, a composite mask was created by combining all constituent regions, and the ROI value was calculated as the mean SUVR across all voxels within the composite mask. The composite mask for meta-temporal ROI was comprised of the entorhinal, amygdala, fusiform, inferior and middle temporal cortices (9). Those regions are used to represent AD-related changes, but it is important to keep in mind that the meta-temporal ROI was optimized on [^{18}F]Tauvid (10, 11). For this reason, we also assessed SUVR within the CenTauR masks (12). Age-related and off-target regions selected were: pallidum, putamen, caudate, thalamus, choroid plexus, meninges, eroded white matter as well as the extracortical hotspot medial to the entorhinal cortex (EntoEch) (4, 13). An individualized meningeal mask was generated in subject space using FreeSurfer-derived segmentations. To capture signal originating from tissue surrounding the cortex, the cortical gray matter mask was expanded outward by a fixed distance of 7 voxels, thereby defining a peripheral layer corresponding to the meninges. The white-matter mask for the white matter region was created by applying an erosion protocol to an initial binary mask derived from Freesurfer-derived white matter and corpus callosum segmentation. To account for scanner resolution, this mask was smoothed using a 6mm^3 kernel. Voxels were subsequently kept if they

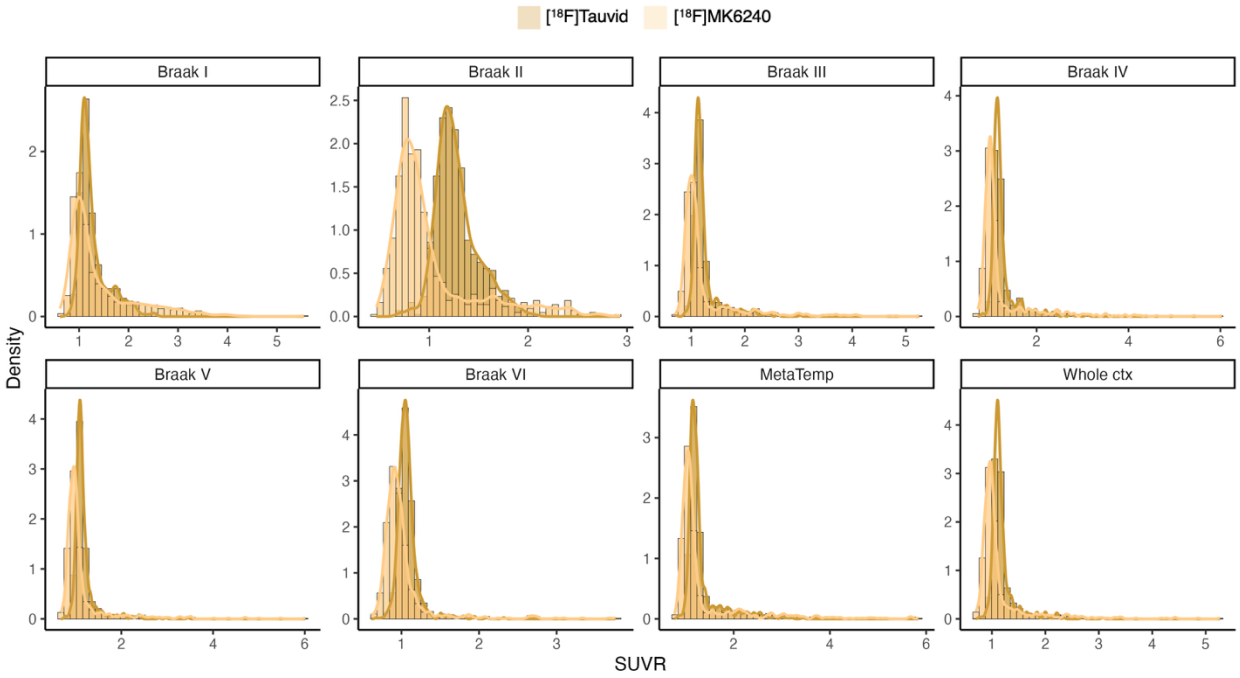
were part of the initial mask and exceeded a density threshold of 0.7 in the smoothed volume, thereby removing voxels prone to partial volume effects from adjacent gray matter or ventricles. This method allows for removal of white matter voxels that would be most impacted by PET partial volume effects from neighboring regions. The MPRAGE was segmented using Freesurfer, with resulting voxelsize 1x1x1mm3, thus for EntoEch, using the Freesurfer segmentation of the left and right entorhinal cortex, the center of mass was calculated between the left and right entorhinal cortices on the coronal slices, that voxel was assigned a value of 1 to create a line running anterior-to-posterior on the coronal slices that included the entorhinal cortex. That binary mask was then smoothed by 25mmx1mmx5mm (25mm is Left to right, 1mm is anterior to posterior, 5mm is inferior to superior). All smoothed voxels with a value of 0.4 or higher were included in the mask. These parameters were used such that the mask did not extend superior or inferior to the entorhinal cortices and did not overlap with the entorhinal cortices. Aβ status was determined based on visual reads performed by two independent raters (Cohen's Kappa = 0.85); disagreements were resolved by consensus review.

Supplementary figures:

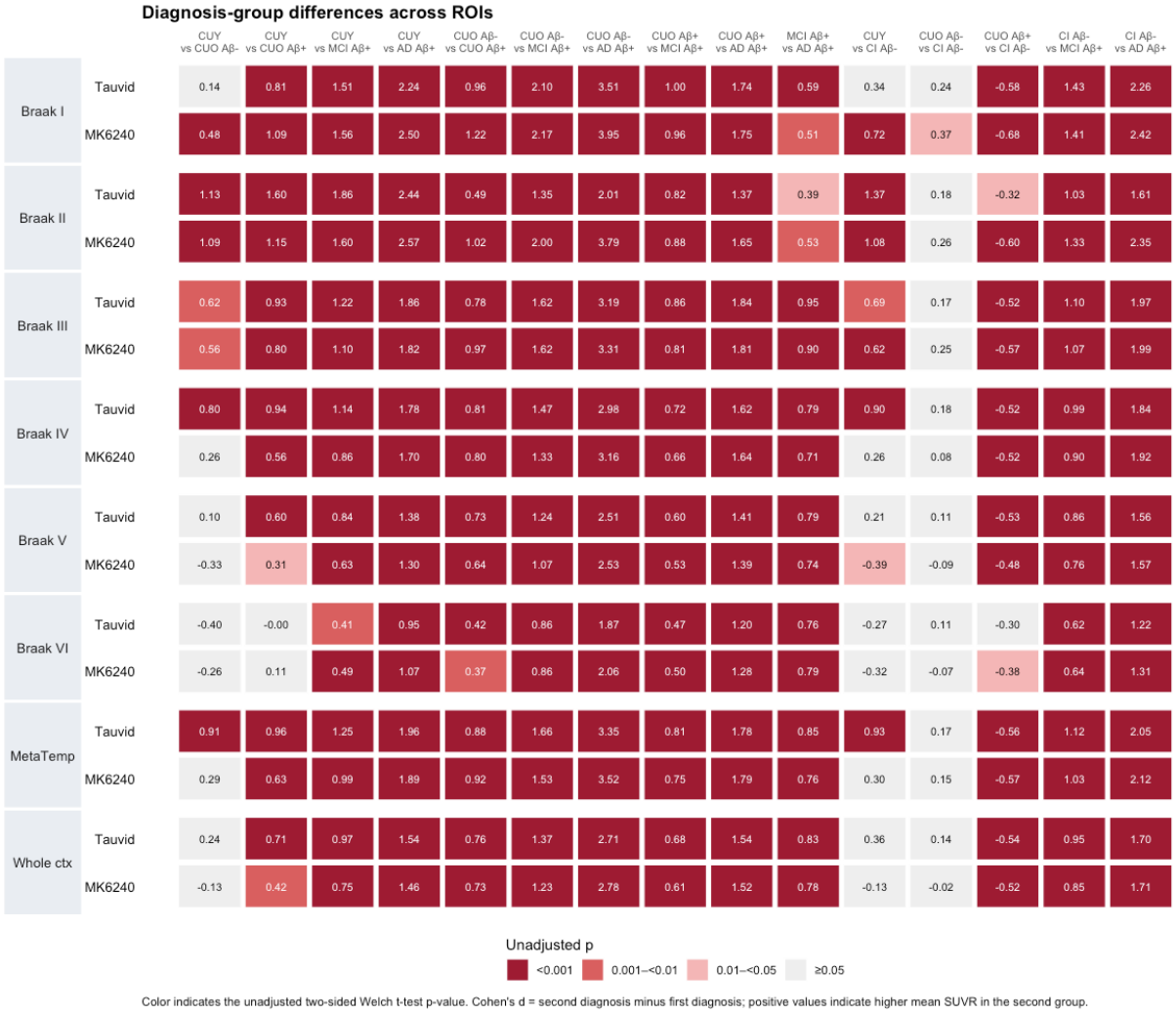
Supplementary figure 1: Standard deviation images of [^{18}F]Tauvid and [^{18}F]MK6240 based on diagnostic group and Aβ status.



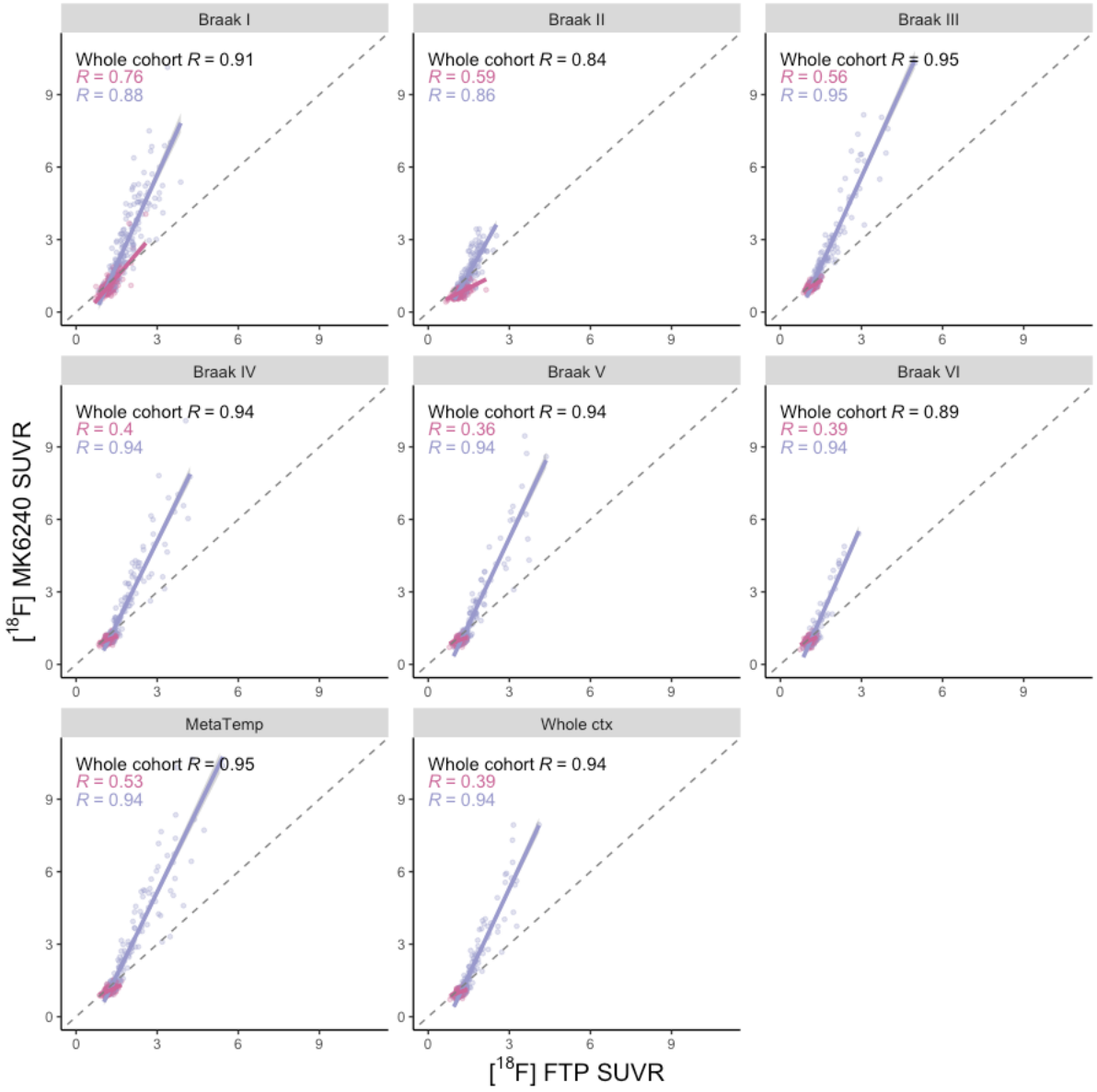
Supplementary figure 2: Histogram of on-target regions



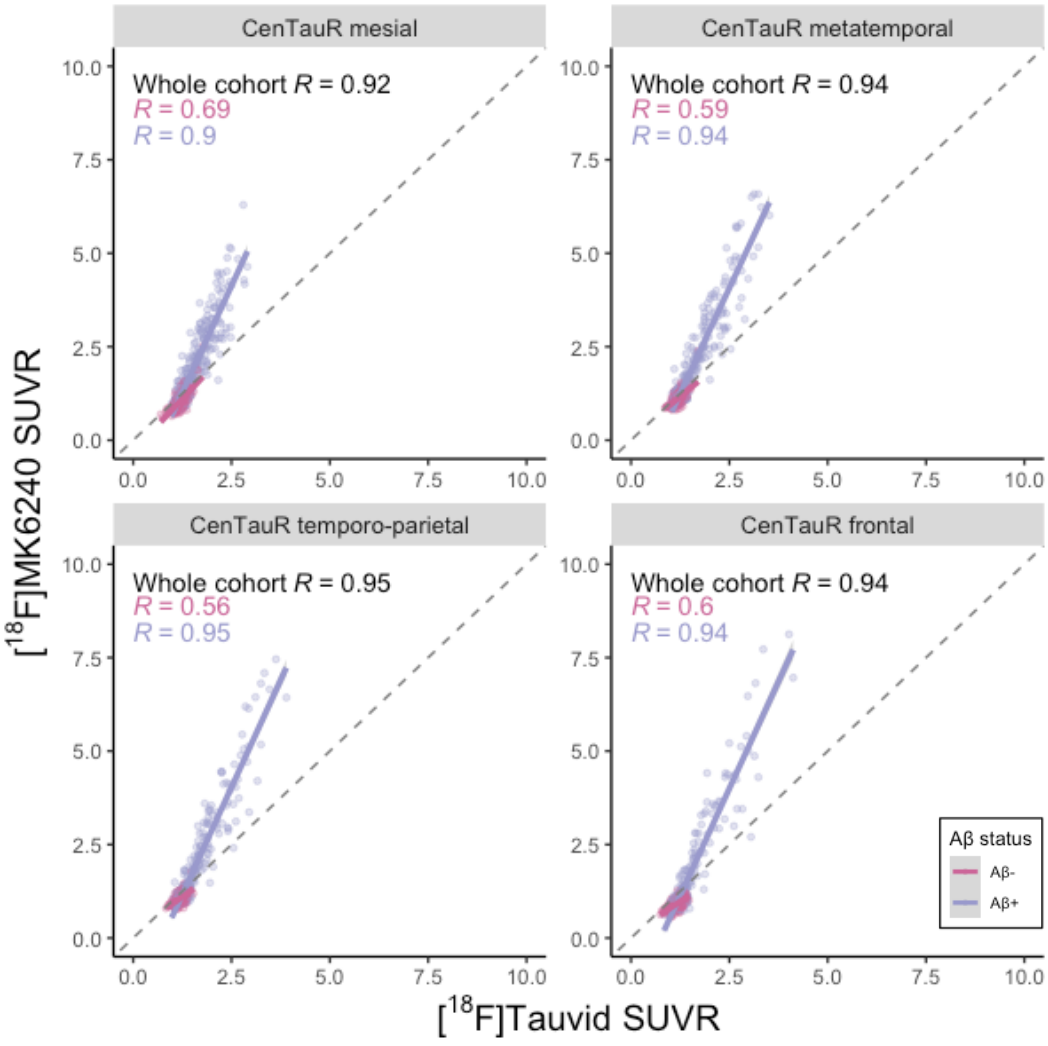
Supplementary figure 3: Diagnosis-group differences across ROIs. Color indicates the significance of t-tests between each diagnostic group in each ROI. Effect sizes are shown in each box, calculated as Cohen's d.



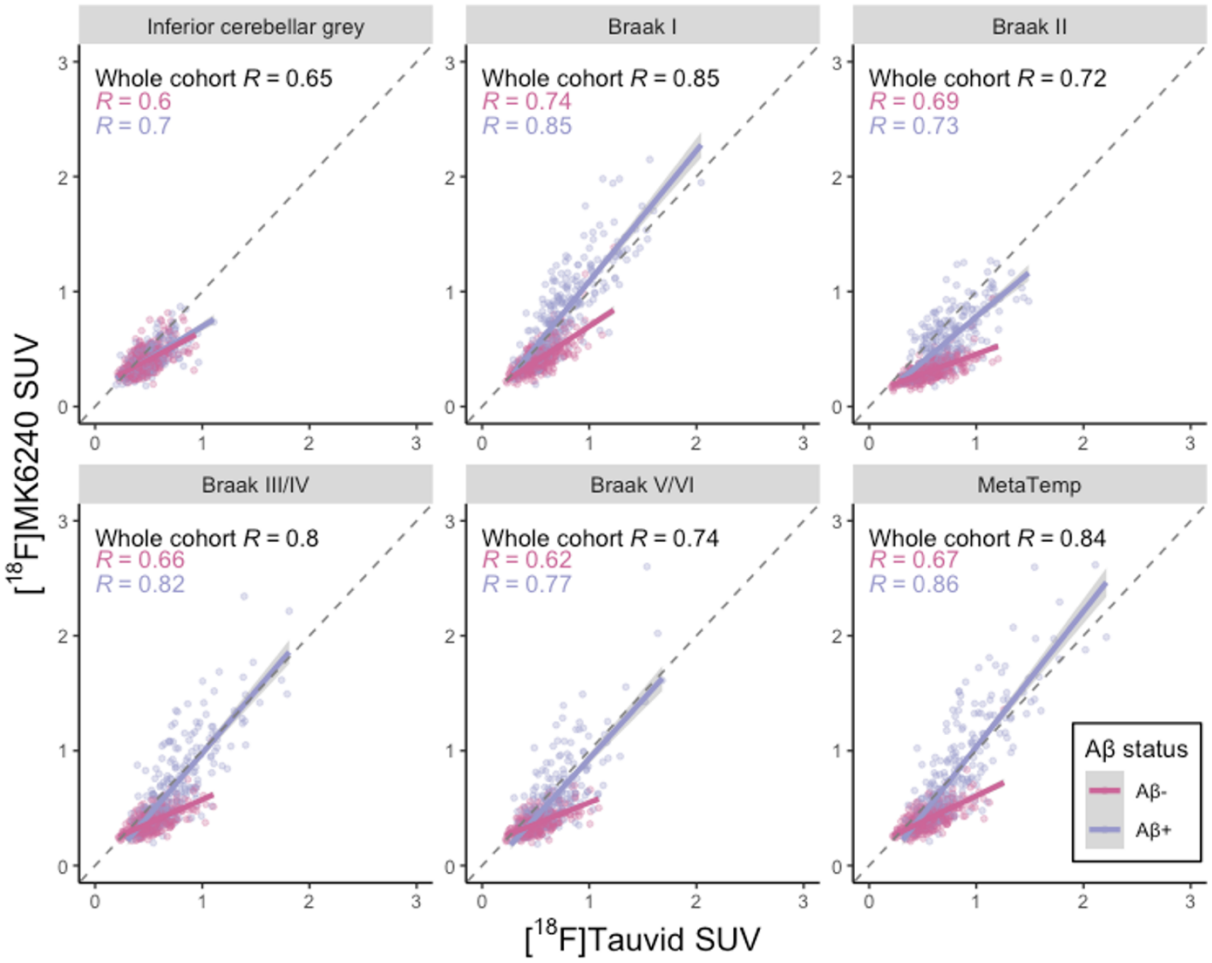
Supplementary figure 4: Associations in partial volume corrected data



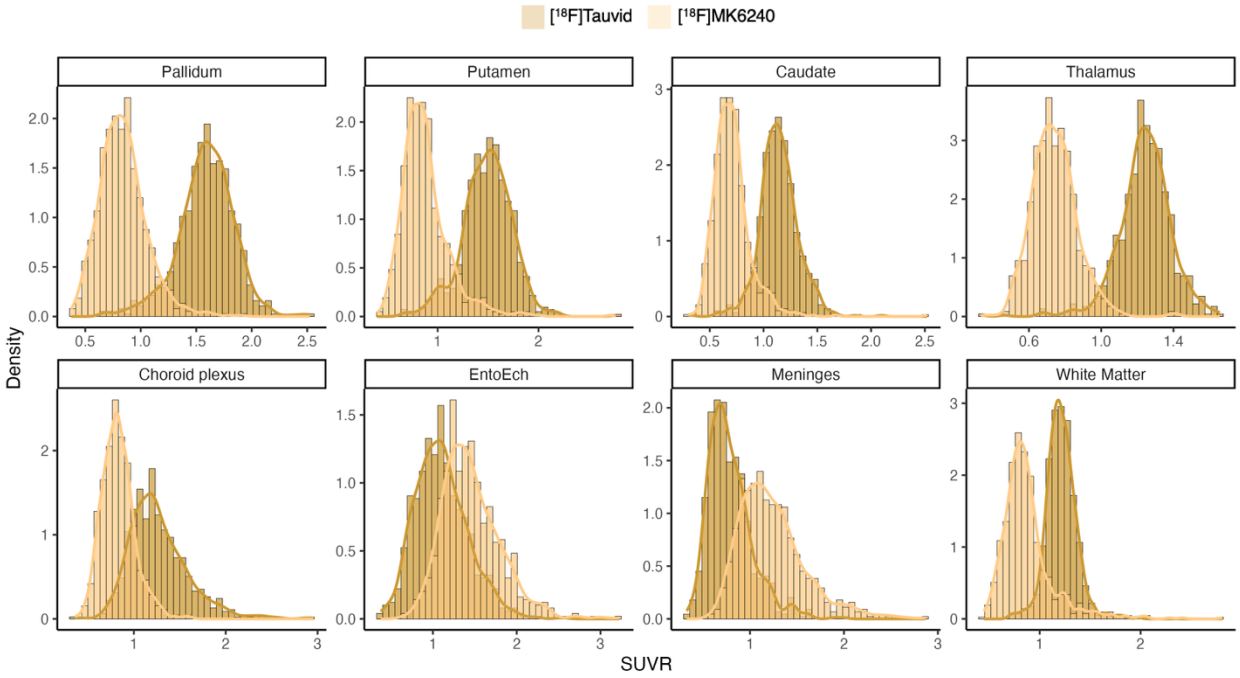
Supplementary figure 5: Associations within CenTauR masks



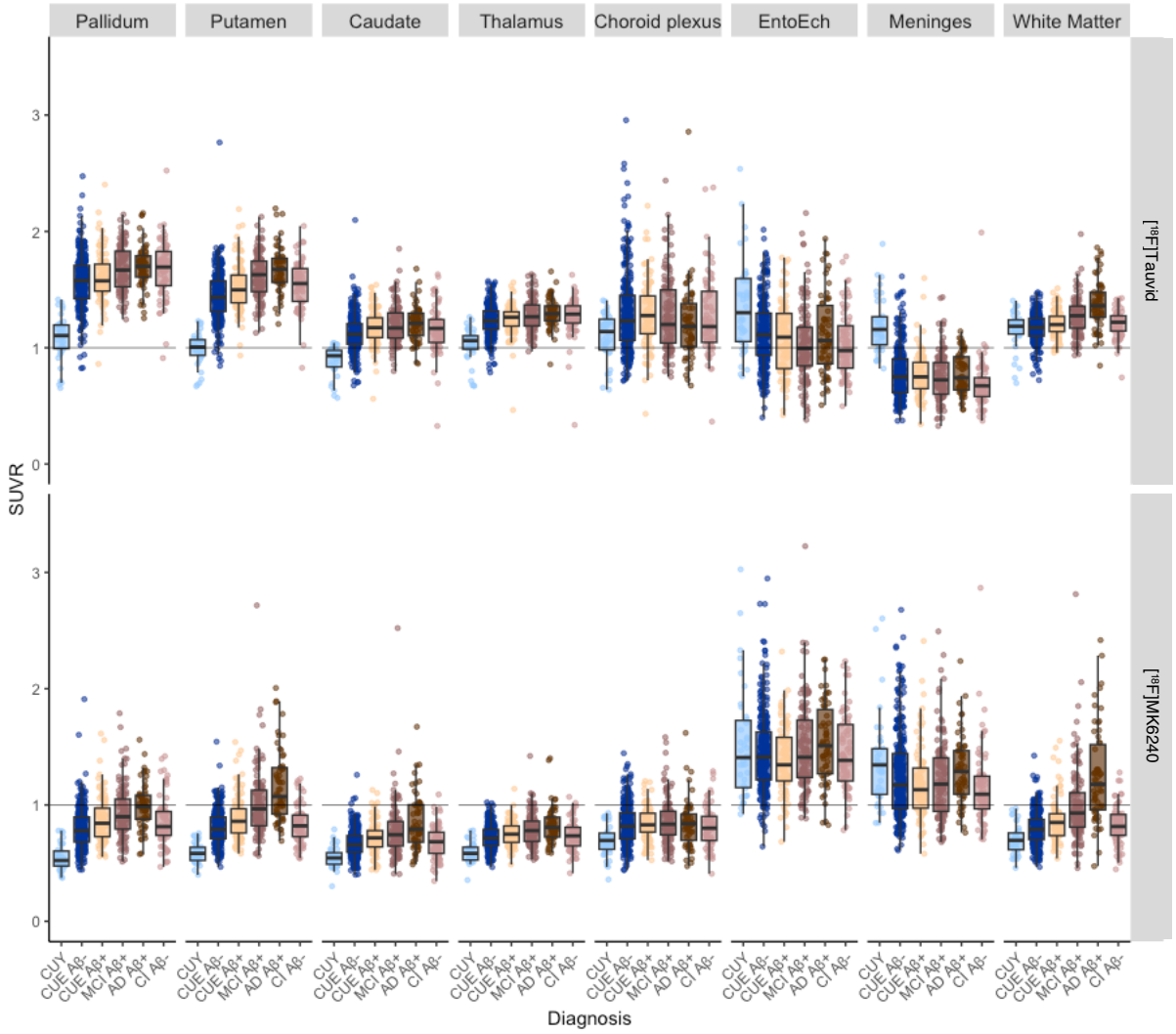
Supplementary Figure 6: SUV correlations between [^{18}F]Tauvid and [^{18}F]MK6240 in reference and on-target regions



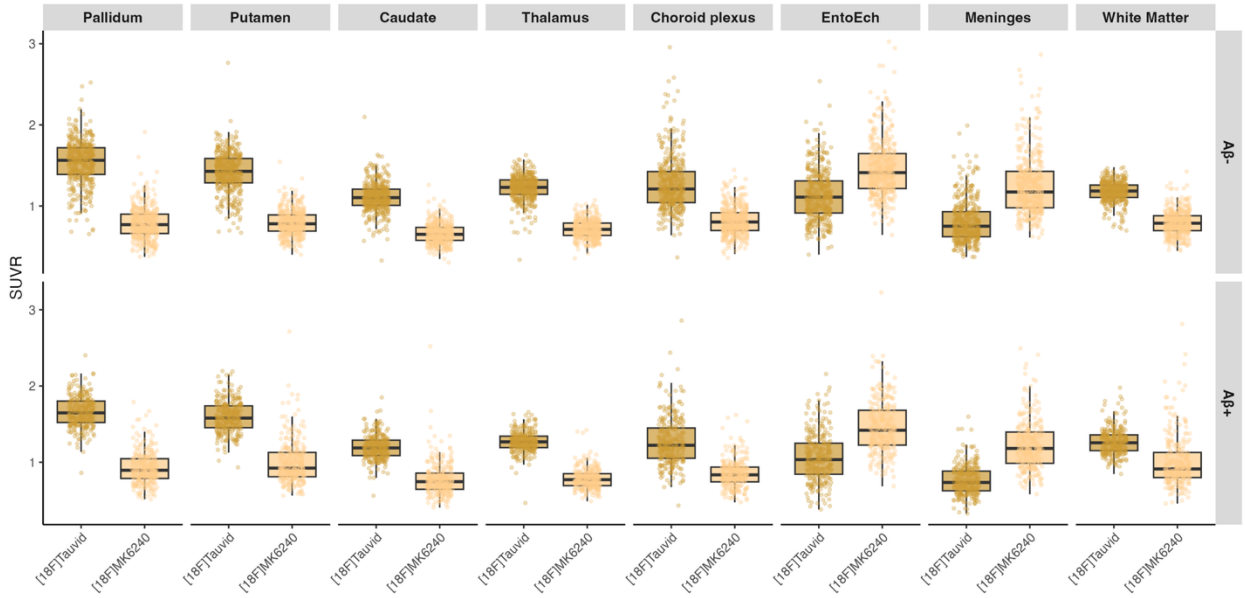
Supplementary figure 7: Histogram of off-target regions



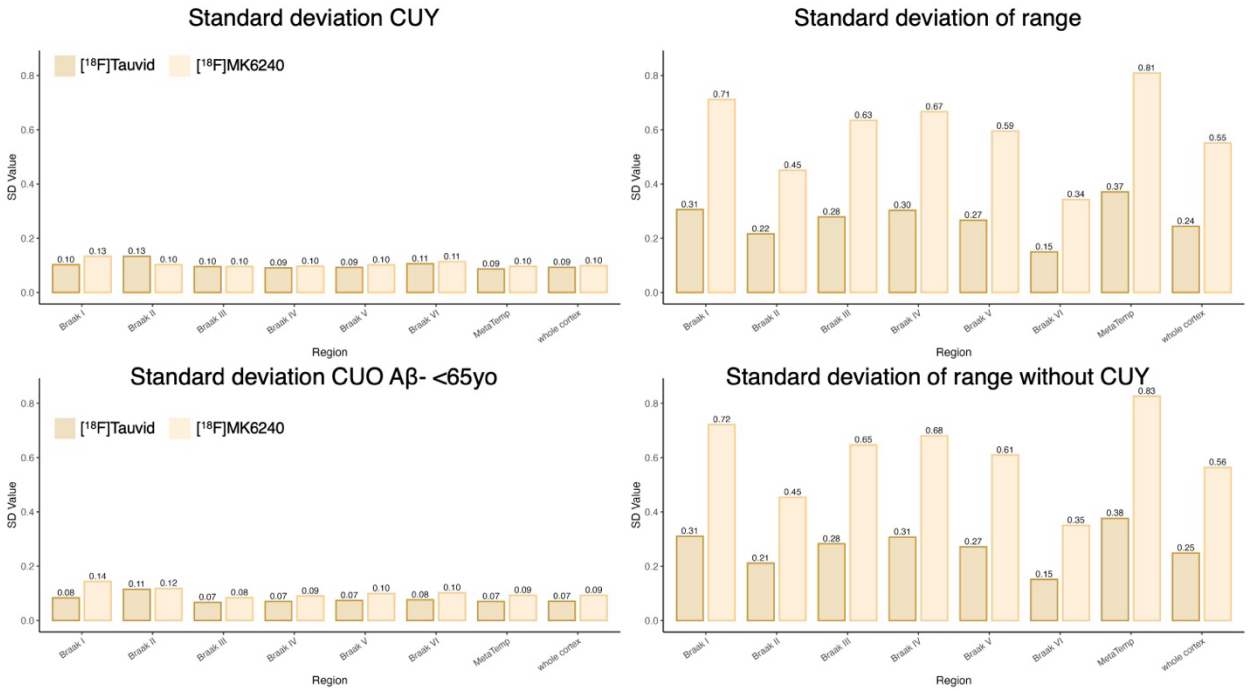
Supplementary figure 8: Boxplot within off-target regions with significant differences. Statistical significance is indicated as p ≤ 0.05 (*), ≤ 0.01 (**), ≤ 0.001 (***), and ≤ 0.0001 (****); non-significant comparisons are not shown.



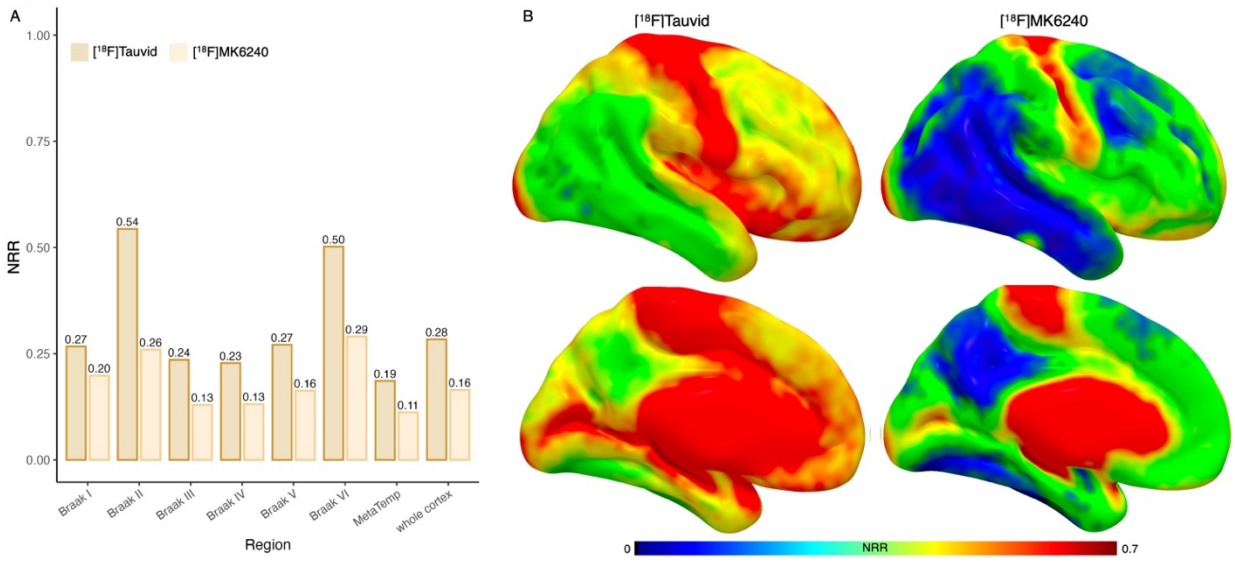
Supplementary figure 9: paired t-test between [^{18}F]Tauvid and [^{18}F]MK6240 in off-target regions. All comparisons were statistically significant $p \leq 0.0001$.



Supplementary figure 10: Standard deviation values of noise and dynamic range used to calculate NRR.



Supplementary figure 11: Noise-to-dynamic range ratio based on CUO Aβ- individuals below 65 years of age.



Supplementary tables:

Supplementary table 1: CI Aβ- individuals demographic information

	CI Aβ- (N=72)
Age (years)	70.5 (8.7)
Aβ-PET burden (Centiloids)	2.9 (6.4)
MoCA total score	24.3 (4.6)

Supplementary table 2: Slopes and intercepts of linear regressions between [^{18}F]Tauvid and [^{18}F]MK6240 in on-target regions.

On-Target Regions Comparison			
Anatomical Region	**Aβ Status**	**Slope (β)**	**Intercept (α)**
Braak I	Aβ-	1.297	−0.403
Braak I	Aβ+	2.089	−1.171
Braak II	Aβ-	0.643	0.027
Braak II	Aβ+	1.932	−1.376
Braak III	Aβ-	0.853	0.033
Braak III	Aβ+	2.176	−1.427
Braak IV	Aβ-	0.758	0.115
Braak IV	Aβ+	2.149	−1.475
Braak V	Aβ-	0.775	0.111
Braak V	Aβ+	2.196	−1.462
Braak VI	Aβ-	0.835	0.048
Braak VI	Aβ+	2.241	−1.397
MetaTemp	Aβ-	0.856	0.047
MetaTemp	Aβ+	2.112	−1.408
Whole ctx	Aβ-	0.766	0.116
Whole ctx	Aβ+	2.212	−1.482

Supplementary table 3: Slopes and intercepts of linear regressions between [^{18}F]Tauvid and [^{18}F]MK6240 in off-target regions.

Off-Target Regions Comparison			
Anatomical Region	**Aβ Status**	**Slope (β)**	**Intercept (α)**
Pallidum	Aβ-	0.518	−0.013
Pallidum	Aβ+	0.641	−0.141
Putamen	Aβ-	0.468	0.129
Putamen	Aβ+	0.857	−0.369
Caudate	Aβ-	0.495	0.112
Caudate	Aβ+	0.792	−0.172
Thalamus	Aβ-	0.480	0.128
Thalamus	Aβ+	0.569	0.061
Choroid plexus	Aβ-	0.319	0.409
Choroid plexus	Aβ+	0.318	0.446
EntoEch	Aβ-	0.654	0.719
EntoEch	Aβ+	0.642	0.775
Meninges	Aβ-	0.930	0.496
Meninges	Aβ+	1.091	0.392
White Matter	Aβ-	0.715	−0.049
White Matter	Aβ+	1.571	−0.987

Supplementary table 4: Percent gain in tau assessment using CUY as the reference group.

	% gain from [^{18}F]MK6240 to [^{18}F]Tauvid
Braak I	-44.1
Braak II	-63.4
Braak III	-56.0
Braak IV	-51.5
Braak V	-50.9
Braak VI	-53.1
MetaTemp	-49.2
Whole ctx	-52.9

Supplementary table 5: Percent gain in tau assessment using CUO Aβ- individuals below 65 years of age as the reference group.

	% gain from [^{18}F]MK6240 to [^{18}F]Tauvid
Braak I	-25.6
Braak II	-52.3
Braak III	-45.0
Braak IV	-42.2
Braak V	-39.8
Braak VI	-42.2
MetaTemp	-39.6
Whole ctx	-42.0

Reference:

1. Jack CR, Jr., Wiste HJ, Therneau TM, Weigand SD, Knopman DS, Mielke MM, et al. Associations of Amyloid, Tau, and Neurodegeneration Biomarker Profiles With Rates of Memory Decline Among Individuals Without Dementia. JAMA. 2019;321(23):2316-25.
2. McKhann GM, Knopman DS, Chertkow H, Hyman BT, Jack CR, Jr., Kawas CH, et al. The diagnosis of dementia due to Alzheimer's disease: recommendations from the National Institute on Aging-Alzheimer's Association workgroups on diagnostic guidelines for Alzheimer's disease. Alzheimers Dement. 2011;7(3):263-9.
3. Pascoal TA, Shin M, Kang MS, Chamoun M, Chartrand D, Mathotaarachchi S, et al. In vivo quantification of neurofibrillary tangles with [(18)F]MK-6240. Alzheimers Res Ther. 2018;10(1):74.
4. Tissot C, Servaes S, Lussier FZ, Ferrari-Souza JP, Therriault J, Ferreira PCL, et al. The Association of Age-Related and Off-Target Retention with Longitudinal Quantification of [(18)F]MK6240 Tau PET in Target Regions. J Nucl Med. 2023;64(3):452-9.
5. Baker SL, Maass A, Jagust WJ. Considerations and code for partial volume correcting [(18)F]-AV-1451 tau PET data. Data Brief. 2017;15:648-57.
6. Landau SM, Harrison TM, Baker SL, Boswell MS, Lee J, Taggett J, et al. Positron emission tomography harmonization in the Alzheimer's Disease Neuroimaging Initiative: A scalable and rigorous approach to multisite amyloid and tau quantification. Alzheimers Dement. 2025;21(1):e14378.
7. Klunk WE, Koeppe RA, Price JC, Benzinger TL, Devous MD, Sr., Jagust WJ, et al. The Centiloid Project: standardizing quantitative amyloid plaque estimation by PET. Alzheimers Dement. 2015;11(1):1-15 e1-4.
8. Braak H, Braak E. Neuropathological stageing of Alzheimer-related changes. Acta Neuropathologica. 1991;82(4):239-59.
9. Jack CR, Jr., Wiste HJ, Weigand SD, Therneau TM, Lowe VJ, Knopman DS, et al. Defining imaging biomarker cut points for brain aging and Alzheimer's disease. Alzheimers Dement. 2017;13(3):205-16.
10. Ossenkoppele R, Rabinovici GD, Smith R, Cho H, Scholl M, Strandberg O, et al. Discriminative Accuracy of [18F]flortaucipir Positron Emission Tomography for Alzheimer Disease vs Other Neurodegenerative Disorders. JAMA. 2018;320(11):1151-62.
11. Pascoal TA, Therriault J, Benedet AL, Savard M, Lussier FZ, Chamoun M, et al. 18F-MK-6240 PET for early and late detection of neurofibrillary tangles. Brain. 2020;143(9):2818-30.
12. Villemagne VL, Leuzy A, Bohorquez SS, Bullich S, Shimada H, Rowe CC, et al. CenTauR: Toward a universal scale and masks for standardizing tau imaging studies. Alzheimers Dement (Amst). 2023;15(3):e12454.
13. Baker SL, Harrison TM, Maass A, La Joie R, Jagust WJ. Effect of Off-Target Binding on (18)F-Flortaucipir Variability in Healthy Controls Across the Life Span. J Nucl Med. 2019;60(10):1444-51.